Organic petrological and geochemical properties of jet from the middle Triassic Mogila Formation, West Bulgaria

ALEXANDER ZDRAVKOV[1,✉], GEORGE AJDANLIJSKY[2], DORIS GROSS[3] and ACHIM BECHTEL[3]

[1]Department of Geology and Exploration of Mineral Resources, University of Mining and Geology "St. Ivan Rilski", 1700 Sofia, Bulgaria;
✉alex_zdravkov@mgu.bg
[2]Department of Geology and Geoinformatics, University of Mining and Geology "St. Ivan Rilski", 1700 Sofia, Bulgaria; g.ajdanlijsky@mgu.bg
[3]Department Angewandte Geowissenschaften und Geophysik, Montanuniversität Leoben, Peter-Tunner-Str. 5, A-8700 Leoben, Austria;
doris.gross@unileoben.ac.at; achim.bechtel@unileoben.ac.at

Abstract: The paper presents the results of the petrographic and organic geochemical studies of a jet sample recovered from a Mid-Triassic carbonate succession from the West Balkan tectonic zone in Bulgaria. Total organic carbon contents (TOC=92 % daf) and high vitrinite reflectance (Ro=1.9 %) indicate semi-anthracite coalification rank. Very high T_{max} (577 °C) and low HI (~10 mg HC/g TOC) further support the overmature organic matter. Extractable organic matter is characterized by high portions of NSO compounds and asphaltenes (>75 %). Hydrocarbons constitute about 20 % and are characterized by the predominance of the saturated hydrocarbons over the aromatics. *n*-Alkanes distribution, dominated by short-chain compounds (*n*-C_{17-18}), is consistent with the woody origin of the jet and the thermal maturity of the organic matter. The predominance of PAHs with condensed structure over their alkylated isomers is considered to be a result of the complex reaction occurring within the organic matrix during the catagenesis, rather than to the presence of combustion-derived organic matter. Based on the distribution of the diterpenoids, a tentative identification of a possible *Voltziales* conifer family source is identified. Low Pr/Ph ratio (0.88) and aryl isoprenoids outline anoxic conditions of jet formation, whereas the presence of organic sulfur compounds and tri-MTTchroman suggest marine depositional environment with normal salinity.

Keywords: Bulgaria, Anisian jet, depositional environment, organic geochemistry, biomarkers.

Introduction

Recently, the occurrence of jet within the early Middle Triassic (Anisian) carbonate succession of Mogila Fm. from the western part of the Balkan tectonic zone in Bulgaria, was noted (Ajdanlijsky et al. 2018). Jet occurs rarely in the sedimentary record and is entirely constrained to Jurassic and Cretaceous rocks (Howarth 1962; Minčev 1978, 1980, 1982; Minčev & Nikolov 1979; Minčev & Šiškov 1986; Suárez-Ruiz et al. 1994 a,b; Bechtel et al. 2001b; Helfík et al. 2001; Marynowski et al. 2011b; Markova et al. 2017). Its formation proceeds through the deposition of drift wood fragments under anoxic conditions. Subsequent impregnation with bituminous substances, generated either within the resin-impregnated woods during maturation (Suárez-Ruiz et al. 1994b; Bechtel et al. 2001b), or derived externally from the surrounding environment (Suárez-Ruiz et al. 1994a) aids organic matter preservation. The molecular composition of the jet could be further influenced by bituminous matter, originating from the bacterial degradation of the organic matter (Bechtel et al. 2001b).

In this paper, the petrographic, bulk geochemical data and molecular composition of the non-polar extract fractions of the jet within the Anisian carbonate succession of Mogila Fm., is reported and used in order to infer its origin and depositional settings.

Geological settings

The Late Alpine Balkan Tectonic zone (Fig. 1a) is characterized by widely distributed Triassic successions, which are part of the main regional tectonic structures and cover lower Palaeozoic high-grade metamorphosed and upper Palaeozoic sedimentary, igneous and volcanic rocks. Stratigraphically, the Triassic rocks are subdivided into three units: i) the Petrohan Terrigenous Group (Tronkov 1981) consisting mainly of fluvial and rare alluvial siliciclastic deposits; ii) the Iskar Carbonate Group (Tronkov 1981) composed of shallow-marine carbonates and mixed siliciclastic-carbonate rocks; and iii) the Moesian Group (Chemberski et al. 1974) represented by terrigenous-carbonate and carbonate rocks. Tronkov (1983) defined four regional stratigraphic levels in the lower part of the Iskar Carbonate Group, i.e. the Tenuis, the Zhitolub, the Sfrazhen and the Sedmochislenitzi Beds (Fig. 1b). The logged interval belongs to the Tenuis Bed from the base of the Iskar Carbonate Group and is situated about 10 m above the base of the Mogila Formation (Opletnya Member; Assereto et al. 1983). Recently, the rocks were chronostratigraphically constrained to the earliest Middle Triassic (Anisian; Ajdanlijsky et al. 2018). Cyclic sedimentary succession of mainly allochemic and mictritic limestone, alternating with dolomitized limestone and dolomite, is the most prominent feature of the Opletnya Member.

High-resolution lithostratigraphic description of the studied section is presented in Figure 1c. The sequence- and cyclo-stratigraphic interpretation followed the concepts proposed by Strasser et al. (1999). The sequence boundaries (SB) were positioned into dolomitic beds with massive to poorly laminated structure, which are considered to represent the shallowest facies deposits. The transgressive surfaces (TS) are erosive, with amplitude in the range 8–10 cm, and mark the beginning of a deepening-up trend. The transgressive deposits (TSd) are composed of massive to trough/planar cross-bedded allochemic to bioclastic limestones and dolo-limestones. Angular to round pebbly to cobble dolo- and limestone intraclasts, forming small lags or occurring along the foresets, are also observed. Well preserved bivalves, gastro- and cephalopod shales can also be recognized. Upwards, nodular to laminated and massive wacke- and mudstones are interbedded by centimeter-thick mainly fine grained beds of mixed carbonate–terrigenous deposits. The maximum-flooding surfaces (mfs) represent the deepest facies and are manifested by increasing bioturbation.

The shallowing-up highstand deposits (HSd) are represented by massive and horizontally laminated, rarely nodular, mud- and wackestones with increasing upwards dolomite content. Up to 5 centimeter-thick (<12 cm) beds with sigmoidal structure and concave up top surface, having lateral extension of <30–40 m, are also common in this part of the elementary sequences.

The thickness of the individual sequences from the Opletnya Member vary from 1.6 to over 4.3 m. Deposition within an unrimmed carbonate platform under peritidal settings is considered by Chatalov (2000).

Tectonically, the area belongs to the eastern part of the West Balkan tectonic zone (Fig. 1a). As part of the Alpine thrust belt the latter suffered multiple collisional and compressional events (in Late Triassic, Mid-Late Jurassic, Mid-Cretaceous, Late Cretaceous and Mid-Eocene) due to the accretion of proximal and exotic continental fragments to Eurasia during the closure of the Tethys ocean (Dabovski et al. 2002).

Material and methods

The studied sedimentary succession is located about 35 km north of the capital city of Sofia, in the vicinity of the Lakatnik Railway Station within the Iskar gorge (43°05'18.2"N, 23°23'01.6"E). Two small jet fragments were noted within a relatively thin (~1.6 m) elementary sequence from the base of the Tenuis Bed (Fig. 1c). The first one represents ~4 cm long and ~0.7 cm thick extraclast within the lower transgressive part of the cycle (Fig. 1c). Because of the small size, however, this jet fragment was not sampled as it would not yield enough material for the analytical procedures. The second jet fragment is consistently larger (15×3 cm) and was recovered from a massive micritic limestone bed just above the maximum flooding surface (Fig. 1c).

For microscopic investigation, three individual fragments (0.5−0.8 mm) of this jet were mounted in epoxy resin, ground and polished. Semi-quantitative maceral analysis was performed on Leica DM 2500P microscope using reflected white and blue excitation light under oil immersion following standard procedures (Taylor et al. 1998). Maceral identification was done after ICCP (1998, 2001). Vitrinite reflectance was measured on 60 points using MIDAS MSP 200 spectrometer, attached to the same microscope. The calibration was done using Spinel (R=0.421 %), YAG (R=0.902 %) and GGG (R=1.716 %) reflectance standards. EDS analyses were performed on JEOL JSM-6010 PLUS/LA scanning electron microscope in order to study the composition of the established ore minerals. SEM was operated at reduced vacuum, back-scattered electron detector and 15 kV accelerating voltage.

The total organic carbon (TOC) and sulphur (S) contents were determined with an Eltra Helios C/S analyzer. Moisture and ash yield were measured following standard procedures (ISO 17246:2010). Rock-Eval pyrolysis was performed using a Rock-Eval 6 instrument. The value of S_2 (mg HC/g rock) was used to calculate the hydrogen index (HI=$100 \times S_2$/TOC [mg HC/g TOC]; Espitalié et al. 1977). The temperature of maximum hydrocarbon generation (T_{max}) was recorded as a maturity parameter.

For GC-MS analysis about 5 g of the jet sample were mixed with inert diatomaceous earth and homogenized. Extraction was performed by a Dionex ASE 200 equipment using dichloromethane for 1 hour at 75 ºC and 75 bar. The extract was concentrated using a Zymark Turbo Vap 500 device. Extract was dissolved in a solvent mixture of hexane:dichloromethane (80:1) and asphaltenes were subsequently separated by centrifugation. The hexane-soluble organic compounds (maltenes) were subdivided into saturated and aromatic hydrocarbons and NSO components using a Köhnen-Willsch MPLC (medium pressure liquid chromatography) instrument (Radke et al. 1980).

The fractions of saturated and aromatic hydrocarbons were analyzed by Thermo-Fisher Trace GC Ultra analyzer, equipped with a 60 m silica capillary column (DB-5MS). Oven temperature was programmed from 40–310 ºC with steps of 4 ºC/min, followed by isothermal period of 30 min. Helium was used as carrier gas. The device was set in electron impact mode with a scan rate of 50−600 Daltons (0.5 sec/scan). The results were processed with the software Thermo-Fisher Xcalibur v.1.4. Identification of biomarkers is based on retention time and comparison of mass spectra with published data. The determination of absolute concentrations of biomarkers was done using internal standards (deuterated n-tetracosane for the aliphatic fraction and 1,1'-binaphthyl for the aromatic fraction) and values were normalized against the total organic carbon contents.

Results and discussion

Petrography and ash yield

The studied jet represent single highly compressed fossil wood fragment, about 15 cm long and about 3 cm thick
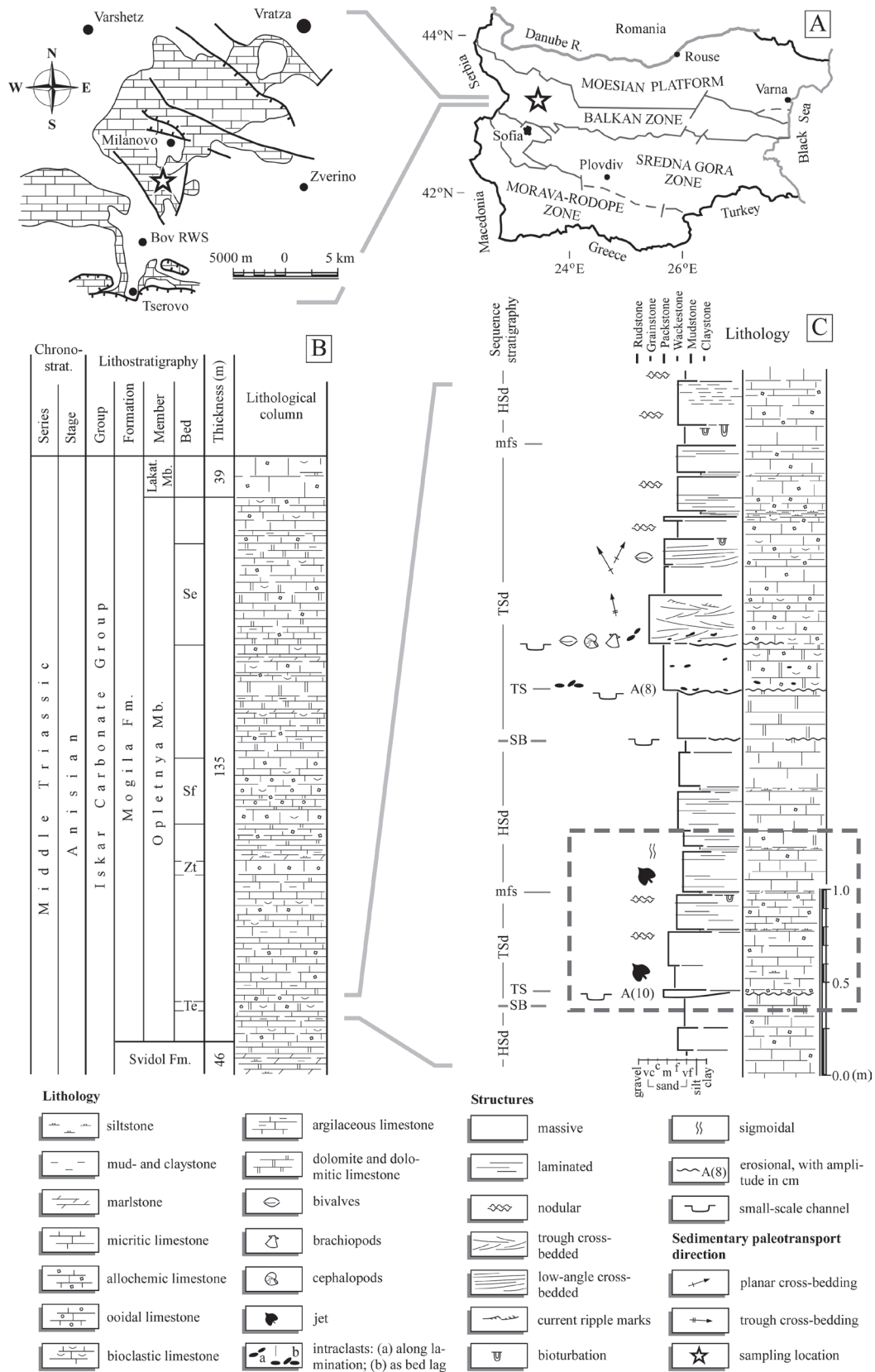
Fig. 1. A — Schematic diagram of the main tectonic units in Bulgaria (simplified after Dabovski et al. 2002) with location of the studied profile. **B** — Lithostratigraphic column of early Mid-Triassic sediments: Te — Tenuis Bed; Zt — Zhitolub Bed; Sf — Sfrazen Bed; Se — Sedmochislenitzi Bed; **C** — high-resolution litho- and cyclostratigraphic log of the studied carbonate succession, showing the position of the jet fragments.

(Fig. 2a). It lies parallel to the bedding, within a thin (20–25 cm) laminated micritic limestone bed, constrained between allo-chemic limestone at the base and allochemic dolomitic lime-stone at the top (Fig. 1). Multiple millimeter sized (<3 mm) carbonate-filled fractures indicate postdepositional deforma-tions of the wood. Micropetrographic investigations revealed strongly gelified organic tissues (V; Fig. 2b–e) significantly fragmented by at least two fracture systems. Neither liptinite nor inertinite macerals were detected. The fractures are mostly filled by carbonate minerals, but some host also pyrite (±pyr-rhotite)−sphalerite hydrothermal mineralization (Fig. 2b,c). The latter is typically constrained to the fractures and only rarely is found within the organic matter (Fig. 2e). Hydro-thermal pyrite always contain certain amount of zinc (pro-bably in the form of micrometer-sized sphalerite inclusions; Fig. 2h), whereas sedimentary pyrite was found to be free of admixtures (Fig. 2i). Based on this observation sedimentary pyrite was tentatively differentiated from the hydrothermal one. Sedimentary pyrite is mostly represented by scarce micrometer-sized euhedral crystals with octahedral and penta-gondodecahedral habit (Fig. 2f,i), scattered within the organic matter (Fig. 2d). Only in one of the studied jet fragments, the presence of several clusters of framboidal and euhedral pyrite was established close to one of the sides of the fragment (Fig. 2f,g), which is assumed to be the outer side of the jet. Following the criteria of Wiese & Fyfe (1986) and Kortenski & Kostova (1996), and considering the co-occurrence of both framboidal and euhedral aggregates, mostly inorganic forma-tion of pyrite can be assumed, although some of the framboids can be also considered of bacterial origin (e.g., Fig. 2g). Fram-boids are typically poorly mineralized, which together with the very low amount of sedimentary pyrite (~0.1 %; Table 1) argue for a limited pyrite formation. Considering the abun-dance of sulfur-containing organic compounds, the negligible pyrite formation indicates iron-deficient marine sedimentary environment.

Vitrinite reflectance measurements (avg. Ro=1.9 %; Table 1) indicate low volatile bituminous to semi-anthracite coalifi-cation stage. However, because of the bituminization, jet is typically characterized by reduced vitrinite reflectance in comparison to coals of same maturity degree (Minčev 1978, 1980; Minčev & Nikolov 1979; Petrova et al. 1985; Minčev & Šiškov 1986; Suárez-Ruiz et al. 1994a,b; Bechtel et al. 2001b). Therefore, in the present case vitrinite reflectance is presumed to be suppressed by the bituminization of the drift wood, and therefore, the actual coalification degree is expected to be higher.

Because of the enhanced postdepositional mineralization, the ash yield of the studied jet is quite high (19 wt. %; Table 1). However, only a small fraction of it is expected to be contri-buted from the living wood. Major elements, like Ca, Mg, Si, Al etc., which play a crucial role in growth or form structural supporting elements in the living tissues, are typically estab-lished in living woods, but generally the total amount of ash do not exceed 0.5 wt. % (Rowell et al. 2005). Although the amount of inorganic matter in the woods vary due to taxonomy and environmental conditions of growth, it is highly unlike that the amount of wood ash in the studied jet sample will be higher than about 2 wt. %. Therefore, it is here assumed that the post-depositional contribution to the jet's ash yield is about 17 %, and all the geochemical parameters were recalculated in order to exclude this contribution.

Bulk geochemical parameters

Bulk organic geochemical parameters, together with the nor-malized yield of extractable organic matter (EOM) and pro-portions of saturated, aromatic and polar compounds and asphaltenes, are summarized in Table 1.

The amount of total organic carbon (TOC) is quite high (92.4 wt. %; Table 1), arguing for a bit higher coalification rank (anthracite) than evidenced from the vitrinite reflectance. Very high T_{max} value of 577 °C (Table 1) suggests overmature organic matter. However, since the amount of hydrocarbons generated during the pyrolysis is quite low (S_2=9.6 mg HC/g rock; Table 1) the high T_{max} might be erroneous. Nevertheless, the very low hydrogen index (HI=10.4 mg HC/g TOC) is consistent with the presence of inert organic matter. Since no inertinite was detected, the low HI unequivocally points towards overmature organic matter outside of the main hydrocarbon generation window. It is therefore possible to assume that the jet was subjected to temperatures over 150 °C. The presence of hydrothermal ore mineralization within the fractured jet suggest that organic matter might have been thermally influenced by the hydrothermal activity. Over 40 small-scale copper and lead-zinc deposits (mostly strata-bound) of presumably Upper Cretaceous age (Campanian–Maastrichtian), exerting strong tectonic control, have been established within the western Balkan orogen (Mincheva-Stefanova 1988). However, the temperatures of main ore formation in one of the biggest Pb–Zn deposits, i.e. "Sedmochislenitsi" deposit (located ~10 km NE of the studied section), most probably did not exceeded 80–100 °C. In addi-tion, no thermal changes can be established within the studied sedimentary sequence, thus suggesting that the temperature of the hydrothermal fluid might have been even lower. On the other hand, Botoucharov (2014) provide data for over-mature (Ro>2 %) organic matter within the Late Triassic rocks at the front of the Balkan thrust zone (southern Moessian Platform margin) in central north Bulgaria. Furthermore, based on subsidence and thermal modelling, the same author indicates that the maximum degree of maturity of the organic matter was achieved by the end of late Aptian, i.e. significantly earlier than the presumed hydrothermal activity. Therefore, considering the complex geodynamic evolution of the Balkan orogen (Dabovski et al. 2002), burial of the sedimentary sequence is here presumed to have exerted the main control on the organic matter maturity.

Total sulfur content was recorded (Table 1), but due to the epigenetic sulfide hydrothermal mineralization and the impossibility to assess its share, the data cannot be inter-preted in terms of environmental settings.
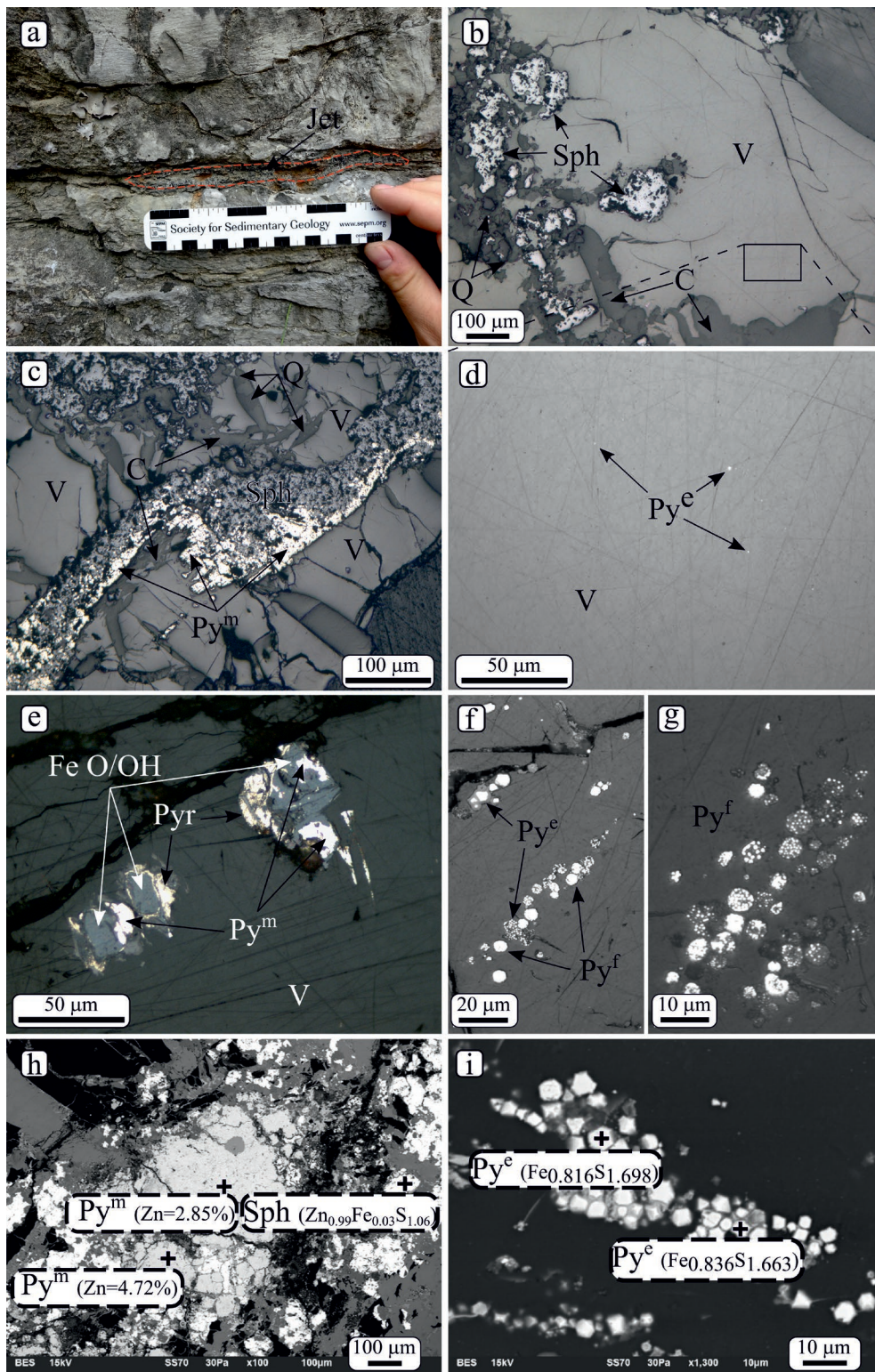
Fig. 2. Petrography of the jet: **a** — macrophotograph showing the position of the jet within the sedimentary sequence; **b, c** — microphotographs showing the complex fragmentation patterns of the jet and the associated hydrothermal ore vein, V=vitrinite, Sph=sphalerite, C=carbonate minerals, Q=quartz, Py^m=massive hydrothermal pyrite; **d** — a close-up microphotograph showing the typical highly gelified organic matter (V) with scarse micrometer sized euhedral pyrite crystals (Py^e), oil immersion; **e** — an example of rare hydrothermal mineralization within the organic matter, Py^m=massive pyrite, Pyr=pyrrhotite, FeO/OH=iron oxides/hydrooxides formed as weathering products of the sulfide minerals; **f, g** — framboidal (Py^f) and euhedral (Py^e) pyrite aggregates, oil immersion; **h** — SEM microphotograph of the hydrothermal vein mineralization with the typical pyrite and sphalerite composition; **i** — SEM microphotograph with composition of euhedral pyrite within the vitrinite. All microphotographs are taken under polarized white light.

Molecular composition of organic matter

The contents of extractable organic matter (EOM) in the studied sample is low (0.4 mg/g TOC; Table 1) and is consistent with the (semi-)anthracite rank of the jet. The EOM is dominated by polar compounds and asphaltenes (Table 1). Predominance of the saturated (15.1 %) over the aromatic hydrocarbons (7.3 %; Table 1) is established.

n-Alkanes and isoprenoids

The total ion current (TIC) chromatogram of the saturated hydrocarbon fraction is shown in Figure 3. The concentrations and proportions of short-, mid- and long-chain *n*-alkanes are presented in Table 2.

The sample is characterized by the presence of *n*-alkanes in the range $n\text{-}C_{15}$ to $n\text{-}C_{33}$ (Figs. 3, 4). The distribution is unimodal and is characterized by the predominance of short-chain hydrocarbons with maximum concentrations at $n\text{-}C_{17\text{-}18}$ (Table 2, Fig. 4a). Prominent peaks at $n\text{-}C_{29}$ and $n\text{-}C_{31}$ (Fig. 4a) point toward the terrestrial origin of the organic matter.

Long-chain *n*-alkanes ($>n\text{-}C_{25}$) are common components of the epicuticular waxes of the vascular plants (Eglinton & Hamilton 1967) and are therefore widely used to infer terrestrial origin of organic matter. On contrary, short-chain homologs ($<n\text{-}C_{20}$) mostly originate from algae and microorganisms (Blumer et al. 1971; Cranwell 1977), whereas mid-chain *n*-alkanes ($n\text{-}C_{21\text{-}25}$) are related to submerged aquatic plants and mosses (Cranwell 1977; Ficken et al. 2000), although bacterial lipids from sulfate-reducing bacteria also contain mid-chain homologs (Han & Calvin 1970). However, *n*-alkane distributions are known to be influenced by bacterial degradation (Allen et al. 1971; Johnson & Calder 1973) and thermal maturation (Tissot & Welte 1984; Peters et al. 2005) of the organic matter. The former results in the progressive removal of the *n*-alkanes, starting with the lighter ones, whereas the latter results in progressive thermal cracking of the long-chain homologs and the formation of shorter-chain *n*-alkanes during maturation. Considering the abundance of short-chain homologs in the studied sample, bacterial degradation of the organic matter is unlike. Furthermore, the trace amounts of hopanes in the studied jet sample do not support the hypothesis of extensive biodegradation. Considering the overmature organic matter, however, thermal cracking of the long-chain hydrocarbons is expected. On the other hand, it has been shown that jet, similarly to other fossil palaeowoods (Fabiańska & Kurkiewicz 2013), is in most cases characterized by short-chain *n*-alkane distribution patterns (Bechtel et

Table 1: Petrographic and organic geochemical characteristics of the studied jet.

Parameter	Value	Units
Ash	19.0	wt. %
Total organic carbon (TOC)	92.4	wt. %
Sulfur	2.7	wt. %
S_2	9.6	mg HC/g rock
Hydrogen Index (HI)	10.4	mg HC/g TOC
T_{max}	577.0	°C
Vitrinite	100.0	vol. %, mmf
Pyrite (sedimentary)	< 0.1	vol. %
Ro	1.9	%
Extractable organic matter	0.4	mg/ g TOC
Σ Saturated HC	15.1	%
Σ Aromatic HC	7.3	%
Σ Polar	40.6	%
Σ Asph.	37.0	%

Table 2: Molecular composition of the aliphatic fraction of the jet extract.

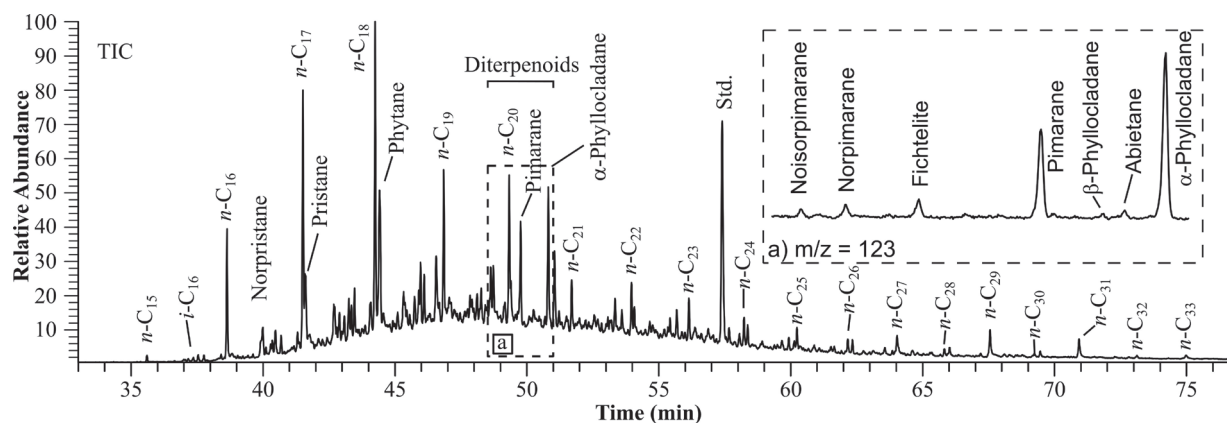|				
Saturated hydrocarbons	**n-Alkanes**	Sum	2.21	µg/g TOC
		$n\text{-}C_{15\text{-}19}$	63.72	%
		$n\text{-}C_{21\text{-}25}$	15.55	%
		$n\text{-}C_{27\text{-}31}$	8.85	%
	Isoprenoids	Sum	0.42	µg/g TOC
		Pr/Ph	0.88	
		Pr/$n\text{-}C_{17}$	0.41	
		Ph/$n\text{-}C_{18}$	0.38	
	Diterpenoids	Sum	0.50	µg/g TOC
		Abietane-type	9.54	%
		Pimarane-type	36.85	%
		Phyllocladane-type	53.61	%
	Regular Steranes	Sum	0.02	µg/g TOC
	Hopanes	Sum	0.02	µg/g TOC

Fig. 3. Gas chromatogram of the saturated hydrocarbon fraction of the jet sample with partial chromatogram of diterpenoids distribution (a). Std.=standard.

al. 2001b; Marynowski et al. 2014; Markova et al. 2017), because of the absence (or the minor amounts) of long-chain fatty acids within the woods, as these are present mainly in the leaf waxes. Considering these facts, the observed unusual *n*-alkane distribution pattern can be attributed mostly to the woody origin of the jet, overprinted by the effects of the thermal maturation of the organic matter.

The studied jet sample is characterized by the presence of low amounts of isoprenoids in the range *i*-C_{16-20}, among which pristane (Pr) and phytane (Ph) are the most abundant (Fig. 3; Table 2). Both commonly originate from the phytyl side chain of chlorophyll-α in photosynthesizing organisms (Peters et al. 2005), whose degradation is strongly controlled by the Eh settings of the depositional environment (Didyk et al. 1978; Volkman & Maxwell 1986). Oxygenated environments are known to favor the formation of pristane, whereas anoxic settings lead to preferential formation of phytane. Following this interpretation and considering the predominance of phytane over pristane and the low Pr/Ph ratio (<1; Table 2) of the studied jet sample, deposition of the drift wood fragments under reducing environment can be suggested. This hypothesis is also supported by the low Pr/*n*-C_{17} and Ph/*n*-C_{18} ratios (Fig. 4b; Table 2). However, the amount of isoprenoids might be influenced by the thermal maturity (Goossens et al. 1984; Volkman & Maxwell 1986; Koopmans et al. 1999; Peters et al. 2005), as well as by the isoprenoid precursors (e.g., pristane formation from tocopherols (Goossens et al. 1984; ten Haven et al. 1987), and phytane formation from bacterial lipids (Volkman & Maxwell 1986; Peters et al. 2005). Considering the high maturity degree of the organic matter, significant rendering of the pristane concentrations due to the thermal evolution of the jet can be expected. In addition, isoprenoid contribution from additional sources cannot be excluded. Nevertheless, the presumed organic matter deposition under anoxic conditions is in agreement with the generally accepted mode of jet formation (e.g., Suárez-Ruiz et al. 1994a; Bechtel et al. 2001b).

Diterpenoids

The studied jet sample is characterized by the presence of low amounts of tri- and tetracyclic saturated diterpenoids (0.5 μg/g TOC; Table 2) with abietane (fichtelite, abietane), pimarane (norisopimarane, norpimarane, *iso*-pimarane), and phyllocladane (α- and β-phyllocladane) skeleton, among which α-phyllocladane and pimarane are dominant (Fig. 3a). Their aromatic counterparts are more abundant (1.20 μg/g TOC; Table 3) and include abietane type hydrocarbons (nor(19)abieta-3,8,11,13-tetraene, nor(19)abieta-8,11,13-triene, dehydroabietane, simonellite, tetrahydro(1,2,3,4)retene, diaromatic totarane, retene), among which simonellite and retene are predominant. Trace amounts of diaromatic totarane-type diterpenoid is also established (Fig. 5a).

Diterpenoid biomarkers are widely distributed in various sedimentary rocks, coal, fossil resins and amber (Simoneit 1977, 1986; Noble et al. 1985, 1986; Sukh Dev 1989; Otto &
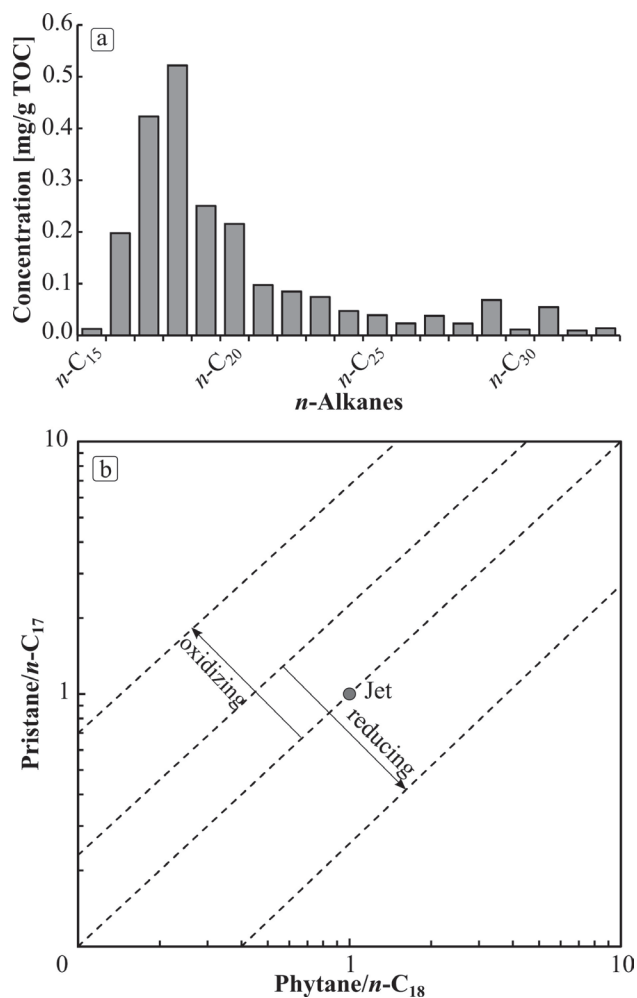
Fig. 4. Histogram, showing the distribution of the *n*-alkanes (**a**) and cross-plot of Phytane/*n*-C_{18} versus Pristane/*n*-C_{17} (**b**) marking the disoxic/anoxic depositional environment.

Table 3: Molecular composition of the aromatic fraction of the jet extract.

Aromatic hydrocarbons	Unsubstituted PAHs	Sum	17.57	μg/g TOC
		Fl/(Fl+Py)	0.44	
		BaA/(BaA+Tri+Ch)	0.15	
		IP/(IP+BgP)	0.41	
	Alkyl-Naphthalenes	MN	0.00	μg/g TOC
		DMN	0.01	μg/g TOC
		TMN	0.09	μg/g TOC
		TeMN	0.44	μg/g TOC
	Alkyl-Phenanthrenes	MP	1.41	μg/g TOC
		DMP	0.15	μg/g TOC
		MPI-1	0.19	
		Rc	2.19	%
	Organic S compounds	DBT	0.85	μg/g TOC
		MDBT	0.66	μg/g TOC
		DMDBT	0.21	μg/g TOC
		BNT	2.28	μg/g TOC
		MDR	12.47	
	Furans		0.05	μg/g TOC
	Diterpenoids		1.20	μg/g TOC
	Aryl isoprenoids		0.46	μg/g TOC
	Chromans		0.01	μg/g TOC

Wilde 2001), and are common constituents of jets (Bechtel et al. 2001b; Marynowski et al. 2014; Markova et al. 2017). Diterpenoids are considered indicators of gymnosperm plants, because of their presence in essential oils and resins. Based on the distribution of the diterpenoid compounds, a general taxonomic differentiation of the different conifer species may be possible (e.g., Simoneit 1977; Wakeham et al. 1980; Noble et al. 1985; Otto & Simoneit 2001; Otto & Wilde 2001). The presence of aromatic abietane type diterpenoids (i.e. simonelite and retene) in recent sediment, however, indicate that aromatization proceeds early in the diagenetic process (Simoneit 1998). Cyclization and aromatization of diterpenoids is known to be mediated by clay mineral catalysts or microbial activity (Wakeham et al. 1980). Furthermore, diterpenoids are thermally unstable and commonly aromatize to retene and eventually to alkyl-phenanthrenes and phenanthrene with increasing rank (Hayatsu et al. 1978). Therefore, considering the high level of thermal maturity of the studied jet, the presence of diterpenoids is surprising. Although the reasons for the occurrence of diterpenoids in this study are currently not fully understood, a combination of a very limited bacterial activity, which correspond to the negligible hopane concentrations, as well as a limited availability of clay mineral catalysts in the carbonate-dominated host rocks, can be considered.

Based on the available geochemical data for the studied jet sample, hardly any specific chemotaxonomic assignment could be done, because of the presence of diterpenoid compounds, characteristic for the whole gymnosperm group. However, it should be noted that the radiation of the modern gymnosperm families (except *Podocarpaceae;* Cleal 1993) from their common ancestors (e.g., *Voltziales* conifers) did not started earlier than the Late Triassic (Cleal 1993; Taylor et al. 2009). Therefore, considering the early Anisian age of the sedimentary succession, it can be assumed that the drift wood most likely originated from the *Voltziales* conifer family. Indirectly, this hypotheses is supported by the establishment of dominant *Voltziales* (e.g., *Voltzia*, *Albertia*, *Yuccites*, *Aethophyllum*) species in the early Anisian red beds of the *Grès à Voltzia* Formation from the western margin of the German Basin. The latter is believed to represent one of the first localities, where the resurgence of the gymnosperms (and particularly the conifers), which survived the harsh arid- to semi-arid conditions following the end-Permian life crisis, have occurred (Grauvogel-Stamm & Ash 2005). On the other hand, Taylor et al. (2009) noted that many of the early conifers share common botanical features with other families, and it can therefore be suggested that this poor differentiation is also expressed in their chemical characteristics.

Steranes and hopanes

Regular steranes and hopanes were detected in equal trace amounts (0.02 μg/g TOC; Table 2), but because of the difficult identification of the individual compounds due to the poor signal-to-noise ratio, their distribution is not discussed here. The very low concentrations of hopanes might indicate a very limited bacterial activity. This is consistent with the presumed coniferous origin of the drift wood, in which resins typically act as anti-bacterial agent. However, both hopanes and steranes are thermally unstable at very high maturity degrees (e.g., Stout & Emsbo-Mattingly 2008) and considering the semianthracite rank of the studied jet this might be the main reason for their general absence.

No rearranged steranes were detected, which is consistent with the dominant carbonate sedimentation during the driftwood deposition. Surprisingly, however, the aromatic fraction does not provide evidence for the presence of neither aromatic steranes, nor hopanes, although their aromatization is known to occur quite early during the diagenesis (Hussler et al. 1984; Peters et al. 2005). However, since the cyclization and aromatization reactions are favored by the catalytic activity of clay minerals, the carbonate-dominated depositional environment might have predetermined their absence.

Polyaromatic hydrocarbons hydrocarbons (PAHs)

The analysis of the aromatics revealed complex composition, characterized by the occurrence and dominance of the unsubstituted three to six rings PAHs, over their alkyl- and phenyl-substituted derivatives (Fig. 5; Table 3). Apart from the abundant phenanthrene, the C_0 PAHs are characterized by predominance of three and four-ring compounds and notable bell-shaped distribution, maximizing at chrysene (Fig. 6).

Predominance of condensed over alkyl-substituted PAHs is often considered to represent contribution from combustion-derived organic matter (e.g., Laflamme & Hites 1978; Wakeham et al. 1980; Yunker et al. 2002). However, such pyrogenic patterns are not uncommon for high-rank coals (semi-anthracite and anthracite) for which rearrangement, fragmentation and condensation reactions during coalification result in progressive loss of alkyl side chains and thus produce significant predominance of the unsubstituted PAHs (e.g., Radke et al. 1982; Wang et al. 2017). The latter is especially pronounced for the two- and three-ring compounds (Chen et al. 2004; Stout & Emsbo-Mattingly 2008). In addition, phenanthrene concentrations in high rank coal can also be increased by demethylation reactions of aromatic diterpenoids (Hayatsu et al. 1987). On the other hand, Bechtel et al. (2001a) report significant increase of phenanthrene concentrations relative to the sum of the methylphenanthrenes, together with abundant sulfur and oxygen heterocyclic hydrocarbons, as a result of demethylation processes related to oxidative hydrothermal alteration of Kupferschiefer Formation near the Rote Fäule zone. Although such explanation for the significant predominance of phenanthrene in the present study seems unlikely given the detected very low concentration of furans (Table 3), the possibility of triphenylene, benz[*b*]fluoranthene, benz[*e*]pyrene formation from dehydrocyclization of alkyl- or phenyl-substituted PAHs (Grafka et al. 2015) cannot be completely excluded as a reason for the decreased methylphenanthrene concentrations. Nevertheless, considering the above discussion, as well as the (semi-) anthracite rank of the studied jet, the established PAHs
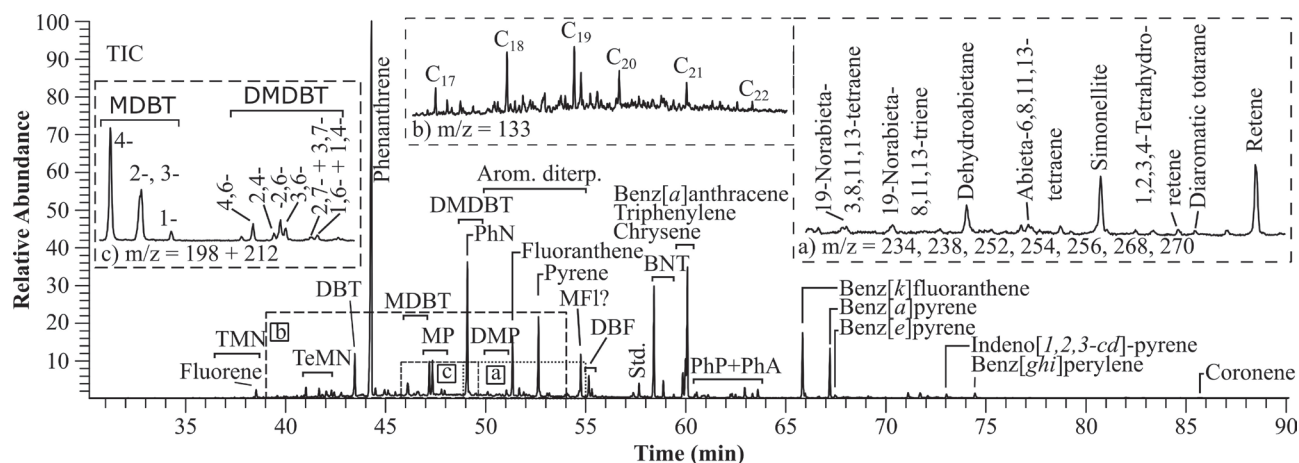
Fig. 5. Gas chromatograms of the aromatic hydrocarbon fraction of the jet sample with partial chromatograms of aromatic diterpenoids (**a**), aryl isoprenoids (**b**) and methyl- and dimethyl-dibenzothiophenes (**c**). TMN=trimethylnaphthalenes; TeMN=tetramethylnaphthalenes; P=phenanthrene; MP=methylphenanthrenes; DMP=dimethylphenanthrenes; DBT=dibenzothiophenes; MDBT=methyldibenzothiophenes; DMDBT=dimethyldibenzothiophenes; DBF=dibenzofurans; BNT=benzonaphthothiophenes; MFl=methylfluoranthene; PhN=phenyl-naphthalene; PhP=phenylphenanthrenes; PhA=phenylanthracenes; Std.=standard.
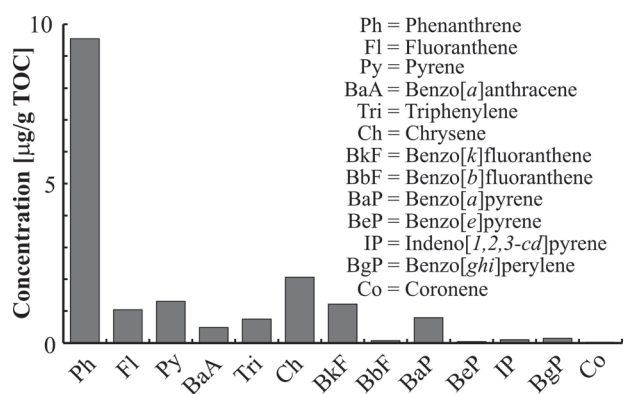

Fig. 6. Distribution of the unsubstituted PAHs.

distribution can mostly be attributed to the thermal transformation reactions within the organic matrix. However, because of the presence of unsubstituted PAHs, which have no apparent biological precursors and are mostly considered to form during burning of organic matter (e.g., pyrene, chrysene, benz[*a*]pyrene, etc.; Fig. 5; Chen et al. 2004; Keiluweit et al. 2012), the possibility of contribution from combustion-derived hydrocarbons should not be completely excluded. In order to evaluate such contribution the ratios Fl/(Fl+Py), BaA/(BaA+Tri+Ch) and In/(In+BgP) (Yunker et al. 2002) were calculated (Table 3). Following the criteria of Yunker et al. (2002) for separation of diagenetically-derived from combustion-deriver PAHs, however, somewhat contradictory conclusions can be drawn. While the ratios Fl/(Fl+Py) and In/(In+BgP) are above the boundaries for diagenetically-derived PAHs (0.4 and 0.2 respectively; Yunker et al. 2002) and thus indicate that minor contribution from pyrolytic organic matter is possible, the low value of the ratio of BaA/(BaA+Tri+Ch) (<0.2; Table 3) is consistent with the absence of such contribution. The results suggest there might be separate sources of

the individual PAHs. As discussed above, the established PAHs distribution is probably mostly a result of the diagenetic and catagenetic transformation of the organic matter. Nevertheless, minor anthropogenic contribution, especially to the five- and six-ring PAHs, should also be taken into account, considering the fact that the studied outcrop is adjacent to a major road and a roadside restaurant.

The alkyl substituted naphthalenes and phenanthrenes are widely used to reflect the thermal maturity of the organic matter. Numerous alkyl-naphthalene and alkyl-phenanthrene ratios have been developed for that purpose (Radke & Welte 1981; Radke et al. 1982, 1986; van Aarssen 1999; Stojanović et al. 2007). Because the observed distribution of the alkyl-naphthalenes is clearly modified by secondary processes (i.e. water washing, oxidation or biodegradation; Volkman et al. 1984; Marynowski et al. 2011a), the methylphenanthrene index (MPI-1; Radke & Welte 1981), which is calibrated and widely used as maturity indicator of Type-III kerogen, was used to further support the maturity assessment of the jet. Following the established empirical relation between MPI-1 and the vitrinite reflectance (Rc=−0.6*MPI-1+2.3; Radke et al. 1984), the calculated methylphenanthrene index (0.19; Table 3) can be correlated to equivalent vitrinite reflectance (Rc) of 2.19 % (Table 3). The value is close to the measured vitrinite reflectance (Ro=1.9; Table 1) and suggest that the suppressing effect that the bituminization play on Ro (e.g., Suárez-Ruiz et al. 1994a,b) might be significantly reduced during maturation, possibly as a result of the transformation of the impregnating resins.

The aromatic fraction is further characterized by the occurrence of sulfur heterocyclic compounds (Fig. 5; Table 3). These are represented by dibenzothiophene and its alkyl-substituted isomers, as well as by benzo[*b*]naphthothiophenes (Fig. 5; Table 3). These compounds have no obvious biological precursors and are therefore considered to originate from

the reaction of the organic matrix with sulfur during early diagenesis (White et al. 1988). Although the mechanisms of sulfur incorporation are still debatable (Wang et al. 2017), it is generally accepted that the origin and distribution of the organic sulfur compounds are controlled by the depositional conditions (Hughes 1984; Hughes et al. 1995) and maturity (Radke et al. 1986). Sediments, deposited in marine environments typically contain increased concentrations of sulfur aromatics, although hypersaline settings in lacustrine basins could also produce such compounds (Hughes et al. 1995; Radke et al. 2000). Owning to the carbonate depositional environment, the presence of sulfur aromatics in the studied jet is not surprising. On the other hand, Radke et al. (1986) pointed out that methyl shifts in the alkyl-dibenzothiophenes follow the same pathway as in the alkyl substituted naphthalenes and phenanthrenes, and based on this proposed the methyldibenzothiophene ratio (MDR) as additional maturity parameter (MDR=4-MDBT/1-MDBT). The distribution of the methyldibenzothiophenes in the examined aromatic extract is clearly dominated by the thermodynamically more stable 4-MDBT (MDR=12.47), which is another proof of the enhanced maturity of the jet's organic matter.

Aryl isoprenoids and chromans

Small amounts (0.46 µg/g TOC; Table 3) of C_{17}–C_{22} aryl isoprenoids with 2,3,6-trimethyl substitution pattern for the aromatic ring and a tail-to-tail isoprenoid chain, were tentatively identified in the aromatic extract fraction (Fig. 5b). The aryl isoprenoids are mostly considered to derive from isorenieratene, which is known to be synthesized by photosynthetic green sulfur bacteria. Since these organisms are phototrophic anaerobes and require both light and H_2S for growth (Pfennig 1977; Summons 1993), the presence of aryl isoprenoids is often interpreted as indication for photic zone anoxia (e.g., Summons & Powell 1987; Sinninghe Damsté et al. 2001). However, Koopmans et al. (1996) report aryl isoprenoids with a 2,3,6-trimethyl substitution as diagenetic transformation products of β-carotene, thus indicating that isorenieratene is not their sole precursor. Considering the very advanced organic matter maturity of the studied jet, the failure to detect isorenieratene, which is typically reported from immature sediments (e.g., Grice et al. 1996; Sinninghe Damsté et al. 2001), is not surprising. Because of this and the absence of carbon isotopic data, however, the detected aryl isoprenoids cannot be equivocally assigned to green sulfur bacteria. Nevertheless, considering the abundance of organic sulfur compounds, arguing for H_2S-rich environment, as well as the anoxic settings, that are prerequisite for jet formation and further evidenced from the low Pr/Ph ratio, at least partial origin of aryl isoprenoids from green sulfur bacteria can tentatively be suggested.

In a series of mono-, di- and trimethylated 2-methyl-2-trimethyltridecylchromans (MTTC; Sinninghe Damsté et al. 1987) only trace amount of the tri-MTTC was tentatively identified in the present study (0.01 µg/gTOC; Table 3).

Despite of the fact that the origin of the methyl substituted MTTCs is still controversial (Sinninghe Damsté et al. 1987, 1993) they are widely used as a palaeosalinity indicator (e.g., Schwark & Püttmann 1990; Grice et al. 1998; Schwark 1998; Bechtel et al. 2013). Empirical evidences (e.g., Sinninghe Damsté et al. 1987, 1993) suggest that formation and preservation of mono-, di- and trimethyl substituted chromans is strongly controlled by the salinity of the depositional environment. Thus non-hypersaline environment favor the synthesis of tri-MTTC, whereas mono-MTTCs are preferentially formed under hypersaline settings. Considering the presence of only tri-MTTC in the studied jet, hypersaline settings seem rather unlike. It is therefore possible to suggest that the deposition and further transformation of the drift wood occurred under normal salinity marine environment. The latter is also supported by the complete absence of gammacerane, which is also widely used to infer hypersalinity (e.g., Jiamo et al. 1986; Sinninghe Damsté et al. 1995; Peters et al. 2005), and is in agreement with the conclusions of Chatalov & Stanimirova (2001) based on the conditions of early diagenetic dolomitization of carbonate mud from Mogila Fm.

Conclusions

Early Mid-Triassic jet, occurring within the cyclic carbonate succession from the lower part of Mogila Formation from the Western Balkan tectonic zone in Bulgaria, was characterized by petrographic analysis, Rock Eval pyrolysis, and organic geochemistry proxies. The results indicate that the jet was formed from wood of vascular plant. The *Voltziales* conifer family seem the most probable source based on the established poor differentiation of the diterpenoid hydrocarbons. High total organic carbon content (TOC=92 %), vitrinite reflectance value (Ro=1.9 %) and T_{max} (577 °C) argue for overmature organic matter at (semi-)anthracite coalification rank. The latter is also well expressed in the molecular composition of the jet. The dominance of short-chain *n*-alkane homologs (*n*-$C_{17–18}$) and the low amounts of the long-chain *n*-alkanes is considered to reflect the woody origin of the jet, overprinted by the enhanced thermal maturity. Furthermore, the predominance of PAHs with condensed structure over their alkylated isomers most probably reflect the complex fragmentation and condensation reactions within the organic matrix during the coalification, rather than the input of combustion-derived organic matter. The calculated equivalent reflectance (Rc=2.14 %), based on the distribution of phenanthrene and methylphenanthrenes, is close to the measured one and further proofs the (semi-)anthracite rank. Because of the timing and the presumed low temperature hydrothermal fluids, the established epigenetic hydrothermal activity is assumed as of negligible influence on the thermal maturity of the organic matter. Therefore, the enhanced maturity of the jet is considered to be a result of the complex geodynamic evolution of the West Balkan tectonic zone and the deep burial of the sediments. The low Pr/Ph ratio (<1), as well as the presence of aryl

isoprenoids, are consistent with drift wood deposition under anoxic environmental settings. Furthermore, the presence of tri-MTTC and the absence of gammacerane argue for normal salinity marine environment of deposition.

References

Ajdanlijsky G., Götz A.E. & Strasser A. 2018: The Early to Middle Triassic continental–marine transition of NW Bulgaria: sedimentology, palynology and sequence stratigraphy. *Geol. Carpath.* 69, 129–148.

Allen J.E., Forney F.W. & Markovetz A.J. 1971: Microbial subterminal oxidation of alkanes and alk-1-enes. *Lipids* 6, 448–452.

Assereto R., Tronkov D. & Ćatalov G. 1983: Mogila Formation (Lower–Middle Triassic) — a new Formation in west Bulgaria. *Geol. Balc.* 13, 25–27 (in Russian).

Bechtel A., Gratzer R., Püttmann W. & Oszczepalski S. 2001a: Variable alteration of organic matter in relation to metal zoning at the Rote Fäule front (Lubin–Sieroszowice mining district, SW Poland). *Org. Geochem.* 32, 377–395.

Bechtel A., Gratzer R. & Sachsenhofer R.F. 2001b: Chemical characteristics of Upper Cretaceous (Turonian) jet of the Gosau Group of Gams/Hieflau (Styria, Austria). *Int. J. Coal Geol.* 46, 27–49.

Bechtel A., Movsumova U., Strobl S.A.I., Sachsenhofer R.F., Soliman A., Gratzer R. & Püttmann W. 2013: Organofacies and paleoenvironment of the Oligocene Maikop series of Angeharan (eastern Azerbaijan). *Org. Geochem.* 56, 51–67.

Blumer M., Guillard R.R.L. & Chase T. 1971: Hydrocarbons of marine phytoplankton. *Mar. Biol.* 8, 183–189.

Botoucharov N. 2014: Vitrinite reflectance, limitations and modelling of oil and gas windows in the central southern part of the Moesian Platform, In: Proceedings of the IV International Scientific and Technical Conference "Geology and Hydrocarbon Potential of the Balkan-Black Sea Region" 11–15. 09. 2013, Varna, Bulgaria. 214–221.

Chatalov A.G. 2000: The Mogila Formation (Spathian–Anisian) in the Western Balkanides of Bulgaria — ancient counterpart of an arid peritidal complex. *Zbl. Geol. Paleont.* Teil-I, 1123–1135.

Chatalov A.G. & Stanimirova T. 2001: Diagenesis of Spathian–Anisian dolomites from the western Balkanides, Bulgaria. *N. Jb. Geol. Palaont. Mh.* 301–320.

Chemberski G., Vaptsarova A. & Monahov I. 1974: Lithostratigraphy of the Triassic variegated terrigenous-carbonate and carbonate sediments studied with deep drilling in Northwestern and Central North Bulgaria. *Ann. DSO Geol. Res* 20, 327–341.

Chen Y., Bi X., Mai B., Sheng G., & Fu J. 2004: Emission characterization of particulate/gaseous phases and size association for polycyclic aromatic hydrocarbons from residential coal combustion. *Fuel* 83, 781–790.

Cleal C.J. 1993: Gymnospermophyta. In: Benton M.J. (Ed.): The Fossil Record 2. *Chapman and Hall, London*, 795–808.

Cranwell P.A. 1977: Organic geochemistry of Cam Loch (Sutherland) sediments. *Chem. Geol.* 20, 205–221.

Dabovski C., Boyanov I., Khrischev K., Nikolov T., Sapunov I., Yanev Y. & Zagorchev I. 2002: Structure and Alpine evolution of Bulgaria. *Geol. Balc.* 32, 9–15.

Didyk B.M., Simoneit B.R.T., Brassell S.C. & Eglinton G. 1978: Organic geochemical indicators of palaeoenvironmental conditions of sedimentation. *Nature* 272, 216–222.

Eglinton G. & Hamilton R.J. 1967: Leaf epicuticular waxes. *Science* 156, 1322–1335.

Espitalié J., Laporte J.L., Madec M., Marquis F., Leplat P., Paulet J. & Boutefeu A. 1977: Méthode rapide de caractérisation des roches mères, de leur potentiel pétrolier et de leur degré d'évolution. *Rev. l'Institut Français du Pétrole* 32, 23–42.

Fabiańska M.J. & Kurkiewicz S. 2013: Biomarkers, aromatic hydrocarbons and polar compounds in the Neogene lignites and gangue sediments of the Konin and Turoszow Brown Coal Basins (Poland). *Int. J. Coal Geol.* 107, 24–44.

Ficken K.J., Li B., Swain D.L. & Eglinton G. 2000: An n-alkane proxy for the sedimentary input of submerged/floating freshwater aquatic macrophytes. *Org. Geochem.* 31, 745–749.

Goossens H., de Leeuw J.W., Schenck P.A. & Brassell S.C. 1984: Tocopherols as likely precursors of pristane in ancient sediments and crude oils. *Nature* 312, 440–442.

Grafka O., Marynowski L. & Simoneit B.R.T. 2015: Phenyl derivatives of polycyclic aromatic compounds as indicators of hydrothermal activity in the Silurian black siliceous shales of the Bardzkie Mountains, Poland. *Int. J. Coal Geol.* 139, 142–151.

Grauvogel-Stamm L. & Ash S.R. 2005: Recovery of the Triassic land flora from the end-Permian life crisis. *Comptes Rendus Palevol* 4, 593–608.

Grice K., Schaeffer P., Schwark L., & Maxwell J.R. 1996: Molecular indicators of palaeoenvironmental conditions in an immature Permian shale (Kupferschiefer, Lower Rhine Basin, north-west Germany) from free and S-bound lipids. *Org. Geochem.* 25, 131–147.

Grice K., Schouten S., Peters K.E., & Sinninghe Damsté J.S. 1998: Molecular isotopic characterisation of hydrocarbon biomarkers in Palaeocene–Eocene evaporitic, lacustrine source rocks from the Jianghan Basin, China. *Org. Geochem.* 29, 1745–1764.

Han J. & Calvin M. 1970: Branched alkanes from blue–green algae. *J. Chem. Soc. D.* 22, 1490–1491.

Hayatsu R., Botto R., Scott R., Mcbeth R. & Winans R. 1987: Thermal catalytic transformation of pentacyclic triterpenoids: Alteration of geochemical fossils during coalification. *Org. Geochem.* 11, 245–250.

Hayatsu R., Winans R., Scott R., Moore L. & Studier M. 1978: Trapped organic compounds and aromatic units in coals. *Fuel* 57, 541–548.

Helfik W., Kwiecińska B., & Zmudzka A. 2001: The occurence of gagate in Soltikow (The Holy Cross Mts.). *Mineral. Pol.* 32, 47–54.

Howarth B.Y.M.K. 1962: The Jet Rock Series and the Alum Shale Series of the Yorkshire coast. *Proc. Yorksh. Geol. Soc.* 33, 381–422.

Hughes W.B. 1984: The use of thiophenic organosulfur compounds in characterizing crude oils derived from carbonate versus siliciclastic source rocks, In: Palacas J.G. (Ed.): Petroleum Geochemistry and Source Rock Potential of Carbonate Rocks. *AAPG Studies in Geology* 18, 181–196.

Hughes W.B., Holba A.G. & Dzou L.I.P. 1995: The ratios of dibenzothiophene to phenanthrene and pristane to phytane as indicators of depositional environment and lithology of petroleum source rocks. *Geochim. Cosmochim. Acta* 59, 3581–3598.

Hussler G., Albrecht P., Ourisson G., Cesario M., Guilhem J. & Pascard C. 1984: Benzohopanes, a novel family of hexacyclic geomarkers in sediments and petroleums. *Tetrahedron Lett.* 25, 1179–1182.

ICCP 1998: The new vitrinite classification (ICCP System 1994). *Fuel* 77, 349–358.

ICCP 2001: The new inertinite classification (ICCP System 1994). *Fuel* 80, 459–470.

ISO 17246:2010: Coal — Proximate analysis.

Jiamo F., Guoying S., Pingan P., Brassell S.C., Eglinton G. & Jigang J. 1986: Peculiarities of salt lake sediments as potential source rocks in China. *Org. Geochem.* 10, 119–126.

Johnson R.W. & Calder J.A. 1973: Early diagenesis of fatty acids and hydrocarbons in a salt marsh environment. *Geochim. Cosmochim. Acta* 37, 1943–1955.

Keiluweit M., Kleber M., Sparrow M.A., Simoneit B.R.T. & Prahl F.G. 2012: Solvent-Extractable Polycyclic Aromatic Hydrocarbons in Biochar: Influence of Pyrolysis Temperature and Feedstock. *Environ. Sci. Technol.* 46, 9333–9341.

Koopmans M.P., Schouten S., Kohnen M.E.L. & Sinninghe Damsté J.S. 1996: Restricted utility of aryl isoprenoids as indicators for photic zone anoxia. *Geochim. Cosmochim. Acta* 60, 4873–4876.

Koopmans M.P., Rijpstra W.I.C., Klapwijk M.M., de Leeuw J.W., Lewan M.D. & Sinninghe Damsté J.S. 1999: A thermal and chemical degradation approach to decipher pristane and phytane precursors in sedimentary organic matter. *Org. Geochem.* 30, 1089–1104.

Kortenski J. & Kostova I. 1996: Occurrence and morphology of pyrite in Bulgarian coals. *Int. J. Coal Geol.* 29, 273–290.

Laflamme R.E. & Hites R.A. 1978: The global distribution of polycyclic aromatic hydrocarbons in recent sediments. *Geochim. Cosmochim. Acta* 42, 289–303.

Markova K., Zdravkov A., Bechtel A. & Stefanova M. 2017: Organic Geochemical characteristics of Bulgarian jet. *Int. J. Coal Geol.* 181, 1–10.

Marynowski L., Kurkiewicz S., Rakociński M., & Simoneit B.R.T. 2011a: Effects of weathering on organic matter: I. Changes in molecular composition of extractable organic compounds caused by paleoweathering of a Lower Carboniferous (Tournaisian) marine black shale. *Chem. Geol.* 285, 144–156.

Marynowski L., Szełęg E., Jędrysek M.O. & Simoneit B.R.T. 2011b: Effects of weathering on organic matter. Part II: Fossil wood weathering and implications for organic geochemical and petrographic studies. *Org. Geochem.* 42, 1076–1088.

Marynowski L., Kubik R., Uhl D. & Simoneit B.R.T. 2014: Molecular composition of fossil charcoal and relationship with incomplete combustion of wood. *Org. Geochem.* 77, 22–31.

Minčev D. 1978: Neue daten über die Hypogenese des Saprovitains (des Gagats) in Zentral-Nordbulgarien. *Annu. l'Universite Sofia "St. Kliment Ohridski", Fac. Geol. Geogr. livre 1 — Geol.* 70, 193–205 (in Bulgarian).

Minčev D. 1980: Der Gagat in der Moesicschen Platte (Bezirk Plewen). *Annu. l'Universite Sofia "St. Kliment Ohridski", Fac. Geol. Geogr. livre 1 — Geol.* 72, 247–268 (in Bulgarian).

Minčev D. 1982: Autochthonity and allochthonity in gagath genesis. *Annu. l'Universite Sofia "St. Kliment Ohridski", Fac. Geol. Geogr. livre 1 — Geol.* 76, 69–78 (in Bulgarian).

Minčev D. & Nikolov Z. 1979: New deposits of saprovitrain (gagate) in Balkan coal Basin. *Annu. l'Universite Sofia "St. Kliment Ohridski", Fac. Geol. Geogr. livre 1 — Geol.* 71, 303–315 (in Bulgarian).

Minčev D. & Šiškov G. 1986: Gagate phytoclast of superhigh microhardness from Low Jurassic sediments in NW Bulgaria. *Annu. l'Universite Sofia "St. Kliment Ohridski", Fac. Geol. Geogr.,* 1, 80, 98–113 (in Bulgarian).

Mincheva-Stefanova J. 1988: Strata-bound polymetalic formation, In: Dimitrov R. (Ed.): Lead and Zinc Deposits in Bulgaria. *Tehnika,* Sofia, 258.

Noble R.A., Alexander R., Kagi R.I. & Knox J. 1985: Tetracyclic diterpenoid hydrocarbons in some Australian coals, sediments and crude oils. *Geochim. Cosmochim. Acta* 49, 2141–2147.

Noble R.A., Alexander R., Kagi R. & Nox J. 1986: Identification of some diterpenoid hydrocarbons in petroleum. *Org. Geochem.* 10, 825–829.

Otto A. & Simoneit B.R.T. 2001: Chemosystematics and diagenesis of terpenoids in fossil conifer species and sediment from the Eocene Zeitz formation, Saxony, Germany. *Geochim. Cosmochim. Acta* 65, 3505–3527.

Otto A. & Wilde V. 2001: Sesqui-, di-, and triterpenoids as chemosystematic markers in extant conifers — A review. *Bot. Rev.* 67, 141–238.

Peters K.E., Walters C.C. & Moldowan J.M. 2005: The Biomarker Guide, Volume 2: Biomarkers and Isotopes in the Petroleum Exploration and Earth History. *Cambridge University Press,* 1–702.

Petrova R., Minčev D. & Nikolov Z. 1985: Comparative investigations on Gagate and Vitrain from the Balkan coal basin. *Int. J. Coal Geol.* 5, 275–280.

Pfennig N. 1977: Phototrophic green and purple bacteria: a comparative, systematic survey. *Annu. Rev. Microbiol.* 31, 275–290.

Radke M. & Welte D.H. 1981: The Methylphenanthrene Index (MPI): A maturity parameter based on aromatic hydrocarbons. In: *Advances in Organic Geochemistry,* 504–512.

Radke M., Willsch H. & Welte D.H. 1980: Preparative hydrocarbon group type determination by automated medium pressure liquid chromatography. *Anal. Chem.* 52, 406–411.

Radke M., Willsch H., Leythaeuser D. & Teichmüller M. 1982: Aromatic components of coal: relation of distribution pattern to rank. *Geochim. Cosmochim. Acta* 46, 1831–1848.

Radke M., Leythaeuser D. & Teichmüller M. 1984: Relationship between rank and composition of aromatic hydrocarbons for coals of different origins. *Org. Geochem.* 6, 423–430.

Radke M., Welte D.H. & Willsch H. 1986: Maturity parameters based on aromatic hydrocarbons: Influence of the organic matter type. *Org. Geochem.* 10, 51–63.

Radke M., Vriend S.P. & Ramanampisoa L.R. 2000: Alkyldibenzofurans in terrestrial rocks: Influence of organic facies and maturation. *Geochim. Cosmochim. Acta* 64, 275–286.

Rowell R.M., Pettersen R., Han J.S., Rowell J.S. & Tshabalala M.A. 2005: Cell Wall Chemistry. In: Rowell R. (Ed.): Handbook of Wood Chemistry and Wood Composites. *CRC Press*, 35–72.

Schwark L. 1998: Geochemical characterization of Malm Zeta laminated carbonates from the Franconian Alb, SW-Germany (II). *Org. Geochem.* 29, 1921–1952.

Schwark L. & Püttmann W. 1990: Aromatic hydrocarbon composition of the Permian Kupferschiefer in the Lower Rhine Basin, N.W. Germany. *Org. Geochem.* 16, 749–761.

Simoneit B.R.T. 1977: Diterpenoid compounds and other lipids in deep-sea sediments and their geochemical significance. *Geochim. Cosmochim. Acta* 41, 463–476.

Simoneit B.R.T. 1986: Cyclic terpenoids of the geosphere, In: Johns R.B. (Ed.): Biological Markers in the Sedimentary Record. *Elsevier,* Amsterdam, 43–99.

Simoneit B.R.T. 1998: Biomarker PAHs in the Environment. In: Neilson A.H. (Ed.): PAHs and Related Compounds. *Springer-Verlag,* Berlin, 175–221.

Sinninghe Damsté J.S., Kock-Van Dalen A.C., De Leeuw J.W., Schenck P.A., Guoying S. & Brassell S.C. 1987: The identification of mono-, di- and trimethyl 2-methyl-2-(4,8,12-trimethyltridecyl)chromans and their occurrence in the geosphere. *Geochim. Cosmochim. Acta* 51, 2393–2400.

Sinninghe Damsté J.S., Keely B.J., Betts S.E., Baas M., Maxwell J.R. & de Leeuw J.W. 1993: Variations in abundances and distributions of isoprenoid chromans and long-chain alkylbenzenes in sediments of the Mulhouse Basin: a molecular sedimentary record of palaeosalinity. *Org. Geochem.* 20, 1201–1215.

Sinninghe Damsté J.S., Frewin N.L., Kenig F., & De Leeuw J.W. 1995: Molecular indicators for palaeoenvironmental change in a Messinian evaporitic sequence (Vena del Gesso, Italy). In: Variations in extractable organic matter of ten cyclically deposited marl beds. *Org. Geochem.* 23, 471–483.

Sinninghe Damsté J.S., Schouten S. & van Duin A.C.. 2001: Isorenieratene derivatives in sediments: possible controls on their distribution. *Geochim. Cosmochim. Acta* 65, 1557–1571.

Stojanović K., Jovančićević B., Vitorovi D., Pevneva G.S., Golovko J.A. & Golovko A.K. 2007: New maturation parameters based on naphthalene and phenanthrene isomerization and dealkylation processes aimed at improved classification of crude oils (Southeastern Pannonian Basin, Serbia). *Geochemistry Int.* 45, 781–797.

Stout S.A. & Emsbo-Mattingly S.D. 2008: Concentration and character of PAHs and other hydrocarbons in coals of varying rank — Implications for environmental studies of soils and sediments containing particulate coal. *Org. Geochem.* 39, 801–819.

Strasser A., Pittet B., Hillgärtner H. & Pasquier J.-B. 1999: Depositional sequences in shallow carbonate-dominated sedimentary systems: concepts for a high-resolution analysis. *Sediment. Geol.* 128, 201–221.

Suárez-Ruiz I., Iglesias M.J., Jiménez A., Laggoun-Défarge F., & Prado J.G. 1994a: Petrographic and Geochemical Anomalies Detected in Spanish Jurassic Jet. In: Vitrinite Reflectance as Maturity Parameter. *American Chemical Society*, 76–92.

Suárez-Ruiz I., Jimenez A., Iglesias M.J., Laggoun-Defarge F. & Prado J.G. 1994b: Influence of Resinite on Huminite Properties. *Energy & Fuels* 8, 1417–1424.

Sukh Dev 1989: Terpenoids, In: Rowe J.W. (Ed.): Natural Products of Woody Plants. *Springer,* Berlin, 691–807.

Summons R.E. 1993: Biogeochemical cycles: a review of fundamental aspects of organic matter formation, preservation, and composition. In: Engel M.H., & Macko S.A. (Eds.): Organic Geochemistry — Principles and Applications. *Plenum Press,* NewYork, 3–21.

Summons R.E. & Powell T.G. 1987: Identification of aryl isoprenoids in source rocks and crude oils: Biological markers for the green sulphur bacteria. *Geochim. Cosmochim. Acta* 51, 557–566.

Taylor G.H., Teichmuller M., Davis A., Diessel C.F.K., Littke R. & Robert P. 1998: Organic petrology. *Gebruder Borntraeger,* Berlin, Stuttgart, 1–704.

Taylor T.N., Taylor E.L. & Krings M. 2009: Paleobotany: The Biology and Evolution of Fossil Plants. Second. Ed., *Elsevier Academic Press*, 1–1253.

ten Haven H.L., de Leeuw J.W., Rullkötter J. & Damsté J.S.S. 1987: Restricted utility of the pristane/phytane ratio as a palaeoenvironmental indicator. *Nature* 330, 641–643.

Tissot B.P. & Welte D.H. 1984: Petroleum Formation and Occurrence. Second Revised and Enlarged Edition. *Springer-Verlag*, 1–720.

Tronkov D. 1981: Stratigraphy of the Triassic System in part of the Western Srednogorie (West Bulgaria). *Geol. Balc.* 11, 3–20 (in Russian).

Tronkov D. 1983: Stratigraphical problems of Iskar Carbonate Group (Triassic) in South-Western Bulgaria. *Geol. Balc.* 13, 91–100 (in Russian).

van Aarssen B.G.K. 1999: Distributions of methylated naphthalenes in crude oils: indicators of maturity, biodegradation and mixing. *Org. Geochem.* 30, 1213–1227.

Volkman J.K. & Maxwell J.R. 1986: Acyclic isoprenoids as biological markers. In: Johns R.B. (Ed.): Biological Markers in the Sedimentary Record. *Elsevier,* Amsterdam, 1–42.

Volkman J.K., Alexander R., Kagi R., Rowland S. & Sheppard P. 1984: Biodegradation of aromatic hydrocarbons in crude oils from the Barrow Sub-basin of Western Australia. *Org. Geochem.* 6, 619–632.

Wakeham S.G., Schaffner C. & Giger W. 1980: Polycyclic aromatic hydrocarbons in Recent lake sediments — II. Compounds derived from biogenic precursors during early diagenesis. *Geochim. Cosmochim. Acta* 44, 415–429.

Wang R., Sun R., Liu G., Yousaf B., Wu D., Chen J. & Zhang H. 2017: A review of the biogeochemical controls on the occurrence and distribution of polycyclic aromatic compounds (PACs) in coals. *Earth-Sci. Rev.* 171, 400–418.

White C.M., Douglas L.J., Schmidt C.E. & Hackett M. 1988: Formation of polycyclic thiophenes from reaction of selected polycyclic aromatic hydrocarbons with elemental sulfur and/or pyrite under mild conditions. *Energy and Fuels* 2, 220–223.

Wiese J.R.G. & Fyfe W.S. 1986: Occurrence of iron sulfides in Ohio coals. *Int. J. Coal Geol.* 6, 251–276.

Yunker M.B., Macdonald R.W., Vingarzan R., Mitchell R.H., Goyette D. & Sylvestre S. 2002: PAHs in the Fraser River basin: A critical appraisal of PAH ratios as indicators of PAH source and composition. *Org. Geochem.* 33, 489–515.